Title

Signalling thresholds and negative B-cell selection in acute lymphoblastic leukaemia



Journal

Nature, 521(7552)

ISSN

0028-0836

Authors

Chen, Zhengshan

Shojaee, Seyedmehdi

Buchner, Maike

et al.

Publication Date

2015-05-01

DOI

10.1038/nature14231

Peer reviewed

Published in final edited form as:

*Nature*. 2015 May 21; 521(7552): 357–361. doi:10.1038/nature14231.

# Signaling thresholds and negative B cell selection in acute lymphoblastic leukemia

**Zhengshan Chen**[1,*], **Seyedmehdi Shojaee**[1,*], **Maike Buchner**[1], **Huimin Geng**[1], **Jae Woong Lee**[1], **Lars Klemm**[1], **Björn Titz**[5], **Thomas G. Graeber**[5], **Eugene Park**[1], **Ying Xim Tan**[4], **Anne Satterthwaite**[6], **Elisabeth Paietta**[7], **Stephen P. Hunger**[8], **Cheryl L. Willman**[9], **Ari Melnick**[10], **Mignon L. Loh**[3], **Jae U. Jung**[11], **John E. Coligan**[12], **Silvia Bolland**[13], **Tak W. Mak**[14], **Andre Limnander**[2], **Hassan Jumaa**[15], **Michael Reth**[16], **Arthur Weiss**[4], **Clifford A. Lowell**[1], and **Markus Müschen**[1]

[1]Department of Laboratory Medicine, University of California, San Francisco, CA 94143

[2]Department of Anatomy, University of California, San Francisco, CA 94143

[3]Pediatric Hematology-Oncology, University of California, San Francisco, CA 94143

[4]Rosalind Russell and Ephraim P. Engleman Arthritis Research Center, Division of Rheumatology, Department of Medicine, Howard Hughes Medical Institute, University of California, San Francisco, CA 94143

[5]Crump Institute for Molecular Imaging, Department of Molecular and Medical Pharmacology, University of California Los Angeles CA

[6]Department of Internal Medicine, University of Texas Southwestern Medical Center, Dallas, TX 75390

[7]Albert Einstein College of Medicine, Bronx, NY 10466

[8]Pediatric Hematology/Oncology/BMT, University of Colorado School of Medicine and Children's Hospital Colorado, Aurora, CO 80045

[9]University of New Mexico Cancer Center, Albuquerque, NM 87102

[10]Departments of Medicine and Pharmacology, Weill Cornell Medical College, New York, NY 10065

[11]Department of Molecular Microbiology and Immunology, University of Southern California, Los Angeles CA

[12]Receptor Cell Biology Section, Laboratory of Immunogenetics, Rockville MD 20852



For correspondence: Markus Müschen, Department of Laboratory Medicine, University of California San Francisco, 521 Parnassus Ave, San Francisco CA 94143, markus.muschen@ucsf.edu.

*Contributed equally to this study.

**Author Contributions**

Z.C. and M.M. designed experiments. M.M. conceived the study. Z.C., S.S., M.B., J.W.L, L.K. and E.P. performed experiments and interpreted data. H.G. performed statistical analysis. Y.X.T, A.S, J.E.C, S.B., T.W.M., M.R. and A.W. provided important reagents and mouse samples. The manuscript was written by Z.C. and M.M. and contributed to by all of the authors.

[13]Autoimmunity and Functional Genomics Section, Laboratory of Immunogenetics, Rockville MD 20852

[14]The Campbell Family Institute for Cancer Research and Ontario Cancer Institute, University Health Network, Toronto, Ontario M5G 2M9, Canada

[15]Department of Immunology, Ulm University, Ulm, Germany

[16]BIOSS Centre for Biological Signalling Studies, and MPI of Immunbiologie and Epigenetics, Albert-Ludwigs-Universität Freiburg, Freiburg, Germany

## Abstract

B cells are selected for an intermediate level of B cell receptor (BCR) signaling strength: Attenuation below minimum (e.g. non-functional BCR)[1] or hyperactivation above maximum (e.g. self-reactive BCR)[2–3] thresholds of signaling strength causes negative selection. In ~25% of cases, acute lymphoblastic leukemia (ALL) cells carry the oncogenic *BCR-ABL1* tyrosine kinase (*Ph*$^+$), which mimics constitutively active pre-BCR signaling[4,5]. Current therapy approaches are largely focused on the development of more potent tyrosine kinase inhibitors to suppress oncogenic signaling *below a minimum* threshold for survival[6]. Here, we tested the hypothesis that targeted hyperactivation *above a maximum* threshold will engage a deletional checkpoint for removal of self-reactive B cells and selectively kill ALL cells. Testing various components of proximal pre-BCR signaling, we found that an incremental increase of Syk tyrosine kinase activity was required and sufficient to induce cell death. Hyperactive Syk was functionally equivalent to acute activation of a self-reactive BCR on ALL cells. Despite oncogenic transformation, this basic mechanism of negative selection was still functional in ALL cells. Unlike normal pre-B cells, patient-derived ALL cells express the inhibitory receptors PECAM1, CD300A and LAIR1 at high levels. Genetic studies revealed that *Pecam1*, *Cd300a* and *Lair1* are critical to calibrate oncogenic signaling strength through recruitment of the inhibitory phosphatases *Ptpn6*[7] and *Inpp5d*[8]. Using a novel small molecule inhibitor of INPP5D[9], we demonstrated that pharmacological hyperactivation of SYK and engagement of negative B cell selection represents a promising new strategy to overcome drug-resistance in human ALL.

---

Acute lymphoblastic leukemia (ALL) represents the most frequent type of cancer in children and is frequent in adults as well. While outcomes for patients with ALL have greatly improved over the past four decades, ALL driven by oncogenic tyrosine kinases (*BCR-ABL1* in adults and other oncogenic fusion tyrosine kinases in childhood ALL)[10] remains a clinical problem. Current efforts to improve treatment options are largely focused on the development of more potent tyrosine kinase inhibitors (TKI). However, responses to TKI are often short-lived. Our group recently identified upregulation of the BCL6 proto-oncogene in response to TKI-treatment as a major mechanism of drug-resistance in *Ph*$^+$ ALL[11]. Here, we propose a strategy to overcome drug-resistance in ALL based on pharmacological hyperactivation of SYK.

Pre-BCR signals are initiated from immunoreceptor tyrosine-based activation motifs (ITAM) in the cytoplasmic tail of Igα (*CD79A*) and Igβ (*CD79B*) signaling chains[12] and essential for survival and proliferation of normal pre-B cells. However, hyperactive

signaling from a self-reactive pre-BCR, owing to ubiquitous presence of self-antigen, induces negative selection and cell death[3]. Here, we observed that *Ph*$^+$ ALL cells consistently lack surface expression of ITAM-bearing signaling chains Igα and Igβ (Extended Data Fig. 1a). Seemingly in contrast to compromised Igα and Igβ expression, multiple components of proximal pre-BCR signaling were activated downstream of the BCR-ABL1 tyrosine kinase (Fig. 1a). These findings demonstrate that oncogenic BCR-ABL1 supplants ITAM-dependent signaling and mimics a constitutively active pre-BCR through engagement with its proximal signaling cascade. Besides BCR-ABL1, mimicry of BCR signaling was previously demonstrated for a number of viral oncoproteins including Epstein–Barr virus latent membrane protein 2A (LMP2A)[13].

Reconstitution of Igα expression induced strong tyrosine phosphorylation of proximal pre-BCR signaling molecules followed by cell death (Extended Data Fig. 1b–d). Likewise, *Ph*$^+$ ALL cells from three patients were highly sensitive to reactivation of ITAM-dependent signaling (LMP2A[13]; Extended Data Fig. 1e–f). Interestingly, activation of ITAM signaling was toxic in leukemic but not normal pre-B cells (Extended Data Fig. 1b). We therefore tested whether BCR-ABL1- and ITAM-dependent activation of proximal pre-BCR signaling are mutually exclusive because both engage the same pre-BCR-associated tyrosine kinases. We therefore repeated activation of ITAM signaling in the presence and absence of TKI-treatment (imatinib; Fig. 1b). Seemingly paradoxically, treatment with imatinib, while designed to kill leukemia cells, rescued *BCR-ABL1* ALL cells in this experimental setting and subsequent washout of imatinib reversed the protective effect (Fig. 1b).

To pinpoint which aspect of proximal pre-BCR signaling is toxic to *Ph*$^+$ ALL cells, we used genetic systems for hyperactivation of Syk, Src and Btk. In contrast to Src and Btk, constitutively active Syk (*Syk*$^{Myr}$) induced rapid cell death (Fig. 1b; Extended Data Fig. 2a–d). Hyperactive Syk was synthetically lethal in combination with oncogenic BCR-ABL1 and cytotoxic effects were mitigated by TKI-treatment (imatinib; Fig. 1b). Like BCR-ABL1, also Syk kinase activity alone mimicked constitutively active pre-BCR signaling and was sufficient to transform mouse pre-B cells (Extended Data Fig. 2e). Interestingly, BCR-ABL1 kinase activity induced phosphorylation of SYK at the interdomain B, which relieves the autoinhibitory conformation of Syk[14]. To study the specific function of SYK interdomain B (Y348 and Y352) tyrosines in *BCR-ABL1* ALL cells, we tested loss (Y→F) and phosphomimetic gain (Y→E) of function mutants of Syk. Empty vectors, kinase-dead Syk$^{K402R}$ and wildtype Syk were used as controls (Fig. 1c). In the absence of constitutive membrane-localization, wildtype Syk had only minor toxic effects on ALL cells. Interestingly, however, expression of Syk carrying phosphomimetic mutations of interdomain B tyrosines (Y348/Y352→E348/E352) induced rapid cell death (Fig. 1c). These findings highlight the relevance of Syk interdomain B tyrosines and suggest that pharmacological approaches to increase tyrosine phosphorylation of the Syk interdomain B may be useful to kill *Ph*$^+$ ALL cells. To study whether Syk tyrosine kinase activity is required for induction of cell death in pre-B ALL cells, we used a Syk tyrosine kinase inhibitor, PRT06207 (PRT). Transduction with constitutively active *Syk*$^{Myr}$ induced rapid cell death, which was rescued by pre-treatment with PRT one day prior to transduction with *Syk*$^{Myr}$ ('PRT-pre'). Interestingly, one day lapse of PRT-treatment and transient

hyperactivation of Syk was sufficient to commit pre-B ALL cells to cell death (Extended Data Fig. 1g).

In the absence of direct strategies for Syk-hyperactivation, we studied pharmacological inhibition of negative regulators of Syk. In normal pre-B cells, activation of Syk downstream of the pre-BCR, is negatively regulated by inhibitory surface receptors that bear immunoreceptor tyrosine-based inhibitory (ITIM)[15] motifs in their cytoplasmic tail. A systematic screen identified 109 ITIM-bearing receptors in the human genome[16], 63 of which are expressed in B cells. Compared to normal pre-B cells and mature B cell lymphoma, the majority of ITIM receptors were upregulated in $Ph^+$ ALL cells. Based on the ratio of expression values in $Ph^+$ ALL compared to pre-B cells and mature B cell lymphoma, PECAM1, CD300A and LAIR1 were identified among the top-ranking ITIM-receptors, which was confirmed by flow cytometry (Extended Data Fig. 3).

To determine whether high expression levels of ITIM-bearing receptors influence the course of human ALL, we segregated patients from two clinical trials (P9906, ECOG 2993) into two groups based on higher or lower than median expression levels of PECAM1, CD300A and LAIR1 at the time of diagnosis. Higher than median expression levels of ITIM receptors on ALL cells at the time of diagnosis predicted shorter overall and relapse-free survival (Extended Data Fig. 4a–e). These findings identify ITIM-bearing inhibitory receptors as a novel biomarker with potential use in risk stratification of children and adults with ALL.

To measure functional consequences of ITIM-receptor deletion, pre-B cells from the bone marrow of *Pecam1*$^{-/-}$, *Cd300a*$^{-/-}$ as well as *Lair1*$^{fl/fl}$ mice and wildtype controls were propagated in the presence of IL7 or transformed with *BCR-ABL1* to model human $Ph^+$ ALL. *Lair1*$^{fl/fl}$ ALL cells were retrovirally transduced with 4-OHT-inducible Cre. Loss of ITIM-receptors had no significant effects on proliferation and survival of normal pre-B cells (Extended Data Fig. 5a). In contrast, in the absence of ITIM-bearing receptors, pre-B ALL cells underwent cellular senescence and cell cycle arrest and failed to form colonies (Fig. 2a; Extended Data Fig. 5a–b) in parallel with activation of cell cycle checkpoint molecules and increased levels of cytoplasmic reactive oxygen species (ROS; Extended Data Fig. 4g–h). Importantly, inducible Cre-mediated ablation of Lair1 surface expression (Extended Data Fig. 4f) resulted in massive hyperactivation of Syk (Y352), SRC kinases (Y416) and Erk (T202/Y204; Fig. 2b), which promotes negative selection of autoreactive B cell clones during early B cell development[17]. In agreement with these findings, Cre-mediated deletion of *Lair1* caused rapid cell death *in vitro*, remission of leukemia *in vivo* and significantly prolonged survival of transplant recipient mice ($P$=0.0003, log rank test; Fig. 2c–d; Extended Data Fig. 5c).

The surface receptors PECAM1, CD300A and LAIR1 attenuate pre-BCR signaling through ITIM-dependent recruitment and activation of inhibitory phosphatases (e.g. PTPN6, INPP5D)[7–8]. For this reason, we performed experiments to determine whether Lair1 contributes to activation of *Ptpn6* and *Inpp5d*. Consistent with a role of Lair1 in recruitment and activation of Ptpn6 and Inpp5d, activating tyrosine phosphorylation of Ptpn6 ($Y^{564}$) and Inpp5d ($Y^{1020}$) was reduced by 3- to 4-fold upon inducible deletion of *Lair1* (Extended Data Fig. 5d). In genetic rescue experiments, we demonstrated that intact ITIM-motifs in the

cytoplasmic tails of Pecam1, Lair1 and Cd300a are critical for the survival of pre-B ALL cells: *Pecam1*$^{-/-}$, *Lair1*$^{-/-}$ and *Cd300a*$^{-/-}$ pre-B cells were transduced with GFP-tagged vectors for reconstitution of Pecam1, Lair1 and Cd300a bearing either wildtype or mutant (Y→F/A) ITIM-motifs or GFP empty vector controls, and then transformed by BCR-ABL1 (Fig. 2e–g). Reconstitution with wildtype-ITIM Pecam1, Lair1 and Cd300a rescued survival and proliferation, whereas reconstitution with receptors carrying tyrosine-mutant ITIMs had no effect (Fig. 2e–g).

The phosphatases PTPN6 (SHP1)[7], INPP5D (SHIP1)[8] and PTPN11 (SHP2)[18] can all bind to ITIM-motifs. We determined their mechanistic contribution to calibration of oncogenic signaling in a genetic rescue experiment: *Lair1*$^{fl/fl}$ ALL cells were transduced with GFP-tagged expression vectors of constitutively active (CA) and phosphatase-inactive forms of Ptpn6, Inpp5d, Ptpn11 (Fig. 3a; Extended Data Fig. 5e). Expression of constitutively active *Inpp5d* and *Ptpn6*, but not *Ptpn11*, rescued Cre-mediated deletion of *Lair1*. Interestingly, inducible deletion of *Ptpn6* or *Inpp5d* was sufficient to cause cell death and a sharp increase of cellular ROS levels in ALL cells (Fig. 3b–c; Extended Data Fig. 6b–e and 7a). Given that phosphatases are sensitive to reversible inactivation by cysteine oxidation of their active sites[19], we tested whether deletion of one single phosphatase triggers a ROS-mediated chain-reaction of phosphatase-inactivation. Using antibodies against phosphatases in inactivated oxidized conformation, we found that deletion of either *Ptpn6* or *Inpp5d* caused wide-spread cysteine-oxidation and inactivation of multiple other phosphatases (Extended Data Fig. 7b). Inducible ablation of *Ptpn6* and *Inpp5d* caused increased expression of Arf and p53 cell cycle checkpoint molecules, $G_{0/1}$ cell cycle arrest and 15- to 40-fold reduced colony formation (Fig. 3d–e; Extended Data Fig. 7c–e). In an *in vivo* transplant experiment, inducible *in vivo* deletion of *Ptpn6* or *Inpp5d* significantly reduced penetrance and extended latency of leukemia (Fig. 3f; $P<0.0005$, log-rank test). These findings reveal a novel and unexpected vulnerability and suggest that ITIM-bearing receptors and inhibitory phosphatases represent a novel class of therapeutic targets in pre-B ALL. Both PTPN6 and INPP5D attenuate ITAM-dependent pre-BCR signaling in normal pre-B cells[7,8]. Cre-mediated depletion of Ptpn6 and Inpp5d protein resulted in strong hyperactivation of Syk ($Y^{352}$; Fig. 3g–h). While PTPN6 directly dephosphorylates ITAMs and SYK[7], INPP5D hydrolyzes the membrane anchor PIP3 and thereby inhibits formation and maintenance of ITAM-dependent signaling complexes at the cell membrane[20]. Pre-treatment with the Syk-inhibitor PRT06207 largely rescued cell death, demonstrating that hyperactivation of Syk is a mechanistic requirement for induction of cell death (Fig. 3i–j).

B-lineage *Ph*$^{+}$ ALL and myeloid lineage chronic myeloid leukemia (CML) are both driven by *BCR-ABL1*. As opposed to *Ph*$^{+}$ ALL, however, defective expression of ITIM-receptors, *Ptpn6* or- *Inpp5d* had no functional consequences in a mouse model for CML (Extended Data Fig. 8 and 9). Consistent with these findings, PTPN6 and INPP5D are highly expressed in patient-derived *Ph*$^{+}$ ALL (n=5) but barely detectable in CML cells (n=5; Extended Data Fig. 6a). To test whether B cell-inherent mechanisms of negative selection are still active and the underlying reason for the divergent behavior of B-lineage and myeloid leukemia, we engineered B cell lineage *Ph*$^{+}$ ALL cells with a doxycycline-inducible vector system for expression of *Cebpa*[21], which results myeloid lineage reprogramming (Extended Data Fig.

10a–b). *BCR-ABL1*-transformed pre-B ALL cells were transduced with GFP-tagged Cre and reprogrammed into myeloid lineage leukemia cells. While inducible ablation of *Lair1*, *Ptpn6* or *Inpp5d* resulted in rapid cell death among B-lineage ($CD19^+$ $B220^+$ $Mac1^-$) ALL cells, myeloid lineage reprogramming ($CD19^-$ $B220^-$ $Mac1^+$) rendered leukemia cells resistant to the effects of inducible deletion (Extended Data Fig. 10c–e). These findings support a scenario in which $Ph^+$ ALL cells are subject to B cell-specific negative selection against hyperactive Syk tyrosine kinase signaling emanating from a self-reactive BCR, or its oncogenic mimic BCR-ABL1. Inducible expression of *Cebpa* subverts B cell lineage commitment and raises the threshold for tyrosine kinase hyperactivation to trigger cell death. In this context, it is interesting to note that multiple genetic lesions in human pre-B ALL target transcription factors that mediate B cell lineage commitment, including *IKZF1*, *PAX5* and *EBF1*[22]. While their mechanistic role is not known, we here propose that deletions of *IKZF1*, *PAX5* and *EBF1*, like downregulation of PAX5 in the context of *Cebpa* expression, reduce stringency of negative selection against hyperactive tyrosine kinase signaling.

A small molecule inhibitor against INPP5D, 3-α-aminocholestane, 3AC[9] (Extended Data Fig. 10f) selectively inhibited enzymatic activity of INPP5D (SHIP1; $IC_{50}$ ~2.5 μmol/l) but not related phosphatases INPP5L1 (SHIP2) and PTEN ($IC_{50}$ >20 μmol/l)[9]. Treatment of patient-derived $Ph^+$ ALL cells with 3AC induced strong hyperactivation of SYK (Fig. 4a). In patient-derived myeloid CML samples, baseline levels of Syk activity were very low and not responsive to 3AC treatment (Extended Data Fig. 10g). Biochemical characterization of 3AC-mediated inhibition of INPP5D in patient-derived $Ph^+$ ALL cells revealed potent and transient hyperactivation of proximal pre-BCR signaling molecules (Fig. 4a). Treatment of patient-derived TKI-resistant $Ph^+$ ALL cells with 3AC induced cell death within four days. Importantly, pre-treatment of $Ph^+$ ALL cells with the SYK-inhibitor (PRT06207) largely protected $Ph^+$ ALL cells against 3AC-induced cell death (Fig. 4b), demonstrating that hyperactivation of Syk is required for induction of cell death. Dose-response analyses revealed that 3AC is selectively toxic for patient-derived $Ph^+$ ALL cells ($IC_{50}$=2.8 μmol/l; n=5) compared to mature B cell lymphoma (n=5; Extended Data Fig. 10h). We next studied drug-responses in a panel of six cases of $Ph^+$ ALL from patients who relapsed under TKI-therapy, including three cases with global TKI-resistance owing to the BCR-$ABL1^{T315I}$ mutation. As expected, treatment with the TKI Imatinib had no effect in BCR-$ABL1^{T315I}$ cases (Extended Data Fig. 10i). In contrast, 3AC induced massive cell death (>95%) in all six cases of $Ph^+$ ALL regardless of *BCR-ABL1* mutation status (Extended Data Fig. 10i). Likewise, treatment of NOD/SCID transplant recipient mice carrying TKI-resistant patient-derived (BCR-$ABL1^{T315I}$) $Ph^+$ ALL cells with 3AC significantly prolonged overall survival ($P$=0.0002, log rank test; Fig. 4c) and reduced leukemia burden (Fig. 4d). While further studies are needed to optimize pharmacological targeting of this pathway, these experiments identify transient hyperactivation of SYK and engagement of negative B cell selection as a powerful new strategy to overcome drug-resistance in $Ph^+$ ALL.

# Methods

## Patient samples and human cell lines

Patient samples (Supplementary Table 1 and 2) were obtained with informed consent in compliance with Institutional Review Board regulations of the University of California San Francisco. Leukemia cells from bone marrow biopsy of patients with $Ph^+$ or $Ph^-$ ALL were xenografted into sublethally irradiated NOD/SCID mice via tail vein injection. After passaging, leukemia cells were harvested and cultured on top of OP9 stroma cells with minimum essential medium (MEMα; Life Technologies) GlutaMAX without ribonucleotides and deoxyribonucleotides, supplemented with 20% fetal bovine serum, 100 IU/ml penicillin, 100 μg/ml streptomycin and 1 mmol/l sodium pyruvate. The human cell lines (Supplementary Table 3) were cultured in RPMI-1640 (Life Technologies) with GlutaMAX containing 20% fetal bovine serum, 100 IU/ml penicillin, and 100 μg/ml streptomycin at 37°C in a humidified incubator with 5% $CO_2$. ALL of the human xenograft cells and cell lines are mycoplasma free.

## Murine cell culture and BCR-ABL1 transformation

Bone marrow cells from constitutive or inducible knockout mice (for a list of genetic mouse models used in this study see Supplementary Table 4) were harvested and cultured in Iscove's modified Dulbecco's medium (IMDM, Invitrogen, Carlsbad, CA) with GlutaMAX containing 20% fetal bovine serum, 50 μM 2-mercaptoethanol, 100 IU/ml penicillin, 100 μg/ml streptomycin in the presence of cytokines. For pre-B cell culture, bone marrow cells were cultured in IMDM with 10 ng/ml recombinant mouse IL-7 (Peprotech, Rocky Hill, NJ) on OP9 stroma cells. For ALL leukemia model, pre-B cells were retrovirally transduced by BCR-ABL1. ALL cells generated from inducible knockout mice were retrovirally transduced with ERT2 or Cre ERT2 virus, and puromycin selection was performed. 4-OHT was used to induce Cre mediated gene deletion. For CML-like leukemia model, the myeloid-restricted protocol described previously was used[23], which generates CML-like cells. Briefly, bone marrow cells were cultured in IMDM with recombinant mouse IL-3 (10 ng/ml), IL-6 (25 ng/ml), SCF (50 ng/ml, PeproTech, Rocky Hill, NJ) and then transformed by BCR-ABL1 retroviurs. Cytokines were removed after BCR-ABL1 transduction.

## *In vivo* transplantation of leukemia cells

Murine pre-B ALL cells transformed by BCR-ABL1 were transduced with firefly luciferase retrovirus, selected with blasticidin, and then transduced with $ER^{T2}$ or Cre $ER^{T2}$ virus, selected with puromycin. 4-OHT was used to induce Cre mediated gene deletion for 24 hours and $1 \times 10^6$ viable cells were injected into sublethally irradiated (250 cGy) NOD/SCID mice via tail vein. For human leukemia cells, a lentiviral vector encoding firefly luciferase was used. Bioimaging of leukaemia progression in mice was performed after transplantation with an in vivo IVIS 100 bioluminescence/optical imaging system (Xenogen). 15 minutes before measuring the luminescence signal, D-luciferin (Promega) prepared in PBS was injected intraperitoneally at an amount of 2.5 mg for each mouse. General anaesthesia was induced by using 5% isoflurane and continued during the process with 2% isoflurane given through a nose cone. When a mouse was terminally sick, it was euthanized and bone marrow and spleen cells were collected for flow-cytometry analysis.

All mouse experiments were subject to institutional approval by the University of California San Francisco Institutional Animal Care and Use Committee. 6–8 week old female NOD-SCID mice were randomly allocated into each treatment group. The minimal number of mice in each group was calculated by using the 'cpower' function in R/Hmisc package. No blinding was used.

### Retroviral and lentiviral transduction

Retrovirus production was performed as described previously[11]. Briefly, transfections of the retroviral constructs together with pHIT60 (gag-pol) and pHIT123 (env) were performed using Lipofectamine 2000 (Invitrogen). 10 mM sodium butyrate was used for induction. The virus supernatant was collected, filtered through a 0.45 μm filter. For lentivirus, PCD/NL-BH (gag-pol) and pMN-VSV-G (env) were used for virus packaging. The lentivirus was concentrated by centricon centrifugal filters from EMD Millipore (Billerica, MA). For transduction, non-tissue culture treated 6-well plates were coated with 50 μg/ml retronectin (Takara, Madison, WI), and virus was loaded by centrifugation (2000 × g, 90 min at 32 °C). Then virus was discarded and $2 \times 10^6$ pre-B cells were transduced per well by centrifugation at 600 × g for 30 minutes. Details of retroviral and lentiviral vectors used were provided in Supplementary Table 5.

### Inhibitors

BCR-ABL1 tyrosine kinase inhibitor Imatinib was obtained from LC Laboratories (Woburn, MA). INPP5D inhibitor 3-α-Aminocholestane (3AC) and *Csk*$^{AS}$ inhibitor 3-IB-PP1 were obtained from EMD Millipore (Billerica, MA). The SYK tyrosine kinase inhibitor PRT062607 was purchased from Selleck Chemicals LLC (Houston, TX).

### Cell viability assay

100,000 human ALL cells were seeded in a volume of 50 μl medium in one well of a 96-well plate (BD Biosciences). Imatinib or any other inhibitor was diluted and incubated at the indicated concentration in a total volume of 100 μl medium. After 3 days, cell counting kit-8 (Dojindo Molecular Technologies) was used to determine the number of viable cells. Fold changes were calculated using baseline values of vehicle treated cells as a reference (set to 100%).

### Flow cytometry

Antibodies used in flow cytometry are mentioned in Supplementary Table 6. For cell-cycle analysis, the BrdU flow cytometry kit (BD Biosciences) or Click-iT EdU Flow Cytometry Assay Kit (Invitrogen) was used according to the manufacturer's instructions. For evaluation of intracellular ROS levels, ALL cells were incubated for 7 min with 1 μM 5-(and 6-)chloromethyl-2′,7′-dichlorodihydrofluorescein diacetate (CM-$H_2$DCFDA, Invitrogen, Carlsbad, CA) at 37°C for oxidation of the dye by ROS. After washing with PBS, the cells were incubated additional 15 min at 37°C in PBS to allow complete deacetylation of the oxidized form of CM-$H_2$DCFDA by intracellular esterases. The levels of fluorescence were then directly analyzed by flow cytometry, gated on viable cells.

### Western blotting

CelLytic buffer (Sigma, St. Louis, MO) supplemented with protease inhibitor cocktail (Roche Diagnostics, IN) and phosphatase inhibitor cocktail set II (EMD Millipore, Billerica, MA) were used to lyse cells. 10 μg of protein lysates per sample were separated on mini precast gels (Bio-Rad, Hercules, CA) and transferred on nitrocellulose membranes (Bio-Rad, Hercules, CA). For the detection of proteins, primary antibodies, alkaline-phosphatase conjugated secondary antibodies, and chemiluminescent substrate (Invitrogen, Carlsbad, CA) were used. Details of primary antibodies were shown in Supplementary Table 7.

### Colony forming assay for mouse cells

10,000 BCR-ABL1-transformed ALL cells or 100,000 CML-like cells were used for this assay. Cells were resuspended in murine MethoCult medium (StemCell Technologies, Vancouver, BC, Canada) and plated on dishes (3 cm in diameter) with an extra dish of water to prevent evaporation. After 7 to 14 days, colonies were counted.

### Senescence-associated β-galactosidase assay

This was performed on cytospin preparations as described previously[11].

### DNA extraction and genotyping

Genomic DNA was extracted from mouse cells with NucleoSpin Tissue kit (MACHEREY-NAGEL, Bethlehem, PA) and PCR was performed by using *Taq* DNA polymerase (NEB, Ipswich, MA). The primer sequences were provided in Supplementary Table 8.

### Gene expression and clinical outcome data

Clinical outcome and gene expression microarray data were derived from the National Cancer Institute TARGET Data Matrix (http://targetnci.nih.gov/dataMatrix/TARGET_DataMatrix.html) of the Children's Oncology Group (COG) Clinical Trial P9906 and from the Eastern Cooperative Oncology Group (ECOG) Clinical Trial E2993. The end points of the clinical data include minimal residual disease (MRD) after 29 days of treatment (COG), overall survival (OS) and relapse-free survival (RFS) probability (COG and ECOG). The detailed information about the gene expression microarray data is provided in Supplementary Table 9 and 10.

### Statistical analysis

Unpaired, two-tailed Student's *t*-test was used to compare colony number, S phase percentage and MFI of ITIM receptors between different groups. Two-sided Mann-Whitney Wilcoxon test was used to compare expression values between $MRD^+$ vs. $MRD^-$ groups. One-sided Mann-Whitney Wilcoxon test was used to compare methylation values of ALL vs. normal pre-B or B-cell lymphoma groups, using R version 2.14.0. OS or RFS probabilities were estimated using the Kaplan-Meier method. Log rank test (two-sided) was used to compare patient survival between different groups. R package "survival" version 2.35–8 was used for the survival analysis. In survival analysis, patients with ALL in each clinical trial (COG P9906 or ECOG E2993) were divided into two groups based on whether their expression was above or below the median level of a probeset or a gene (i.e., the

average of multiple probe sets for a gene). For a multiple-gene predictor (i.e., a set of genes, such as in ITAM (*CD79A*, *CD79B*, *IHGM*) and ITIM (*PECAM1*, *LAIR1*, *CD300A*), the patients were split into 4 groups based on whether they had above or below the median expression levels of the sum of ITAM and the sum of ITIM gene expression levels: i) $ITAM^{High}ITIM^{Low}$ (>= $ITAM_{median}$ and < $ITIM_{median}$), ii) $ITAM^{High}ITIM^{High}$ (>= $ITAM_{median}$ and >= $ITIM_{median}$), iii) $ITAM^{Low}ITIM^{Low}$ (< $ITAM_{median}$ and < $ITIM_{median}$), and iv) $ITAM^{Low}ITIM^{High}$ (< $ITAM_{median}$ and >= $ITIM_{median}$). Survival probability of the $ITAM^{High}ITIM^{Low}$ vs. $ITAM^{Low}ITIM^{High}$ groups in the multiple-gene survival analysis were compared.

## Extended Data

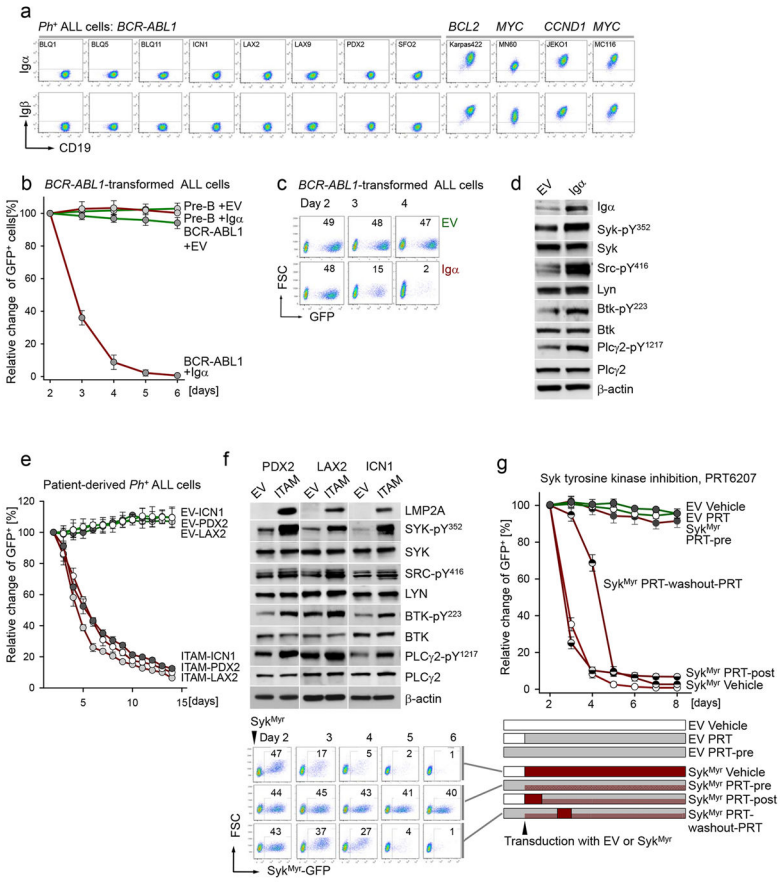


**Extended Data Figure 1. Reconstitution of ITAM signaling causes cell death in pre-B ALL**

**a,** Flow cytometry staining for cell surface Igα (CD79A) and Igβ (CD79B) was performed for patient-derived $Ph^+$ ALL cases (n=8) and B cell leukemia/lymphomas lacking oncogenic tyrosine kinases (n=4). **b–c,** Normal mouse pre-B cells or BCR-ABL1-transformed pre-B ALL cells were retrovirally transduced with CD8-Igα-GFP or empty vector (GFP) controls (EV). Relative changes of transduced ($GFP^+$) populations were monitored by flow cytometry. **d,** Tyrosine phosphorylation of Syk, Src/Lyn, Btk and Plcγ2 was studied in *BCR-ABL1* ALL cells that were transduced with Igα-GFP or GFP empty vector controls, using β-actin as loading control. Data (**c–d**) are representative of three independent experiments. **e,**

Human $Ph^+$ ALL cells were transduced with GFP-tagged vectors for LMP2A-ITAM or EV. Relative changes of transduced ($GFP^+$) populations were monitored by flow cytometry (n=3). **f,** LMP2A-ITAM or an EV was expressed in three cases of human $Ph^+$ ALL cells and effects on LMP2A expression and phosphorylation of SYK, SRC, BTK, PLCg2 were measured by Western blot (n=3). **g,** *BCR-ABL1* transformed ALL cells were transduced with GFP-tagged $Syk^{Myr}$ or an EV, and these cells were treated with the SYK inhibitor PRT06207 (2.5 μmol/l) or vehicle either one day before transduction (PRT-pre), or one day after transduction (PRT-post), or pre-treated, then washed out for one day after transduction, and treated again with PRT. The relative changes of transduced ($GFP^+$) cells were monitored by flow cytometry. Error bars represent mean ± s.d. from three independent experiments (**b, e, g).**

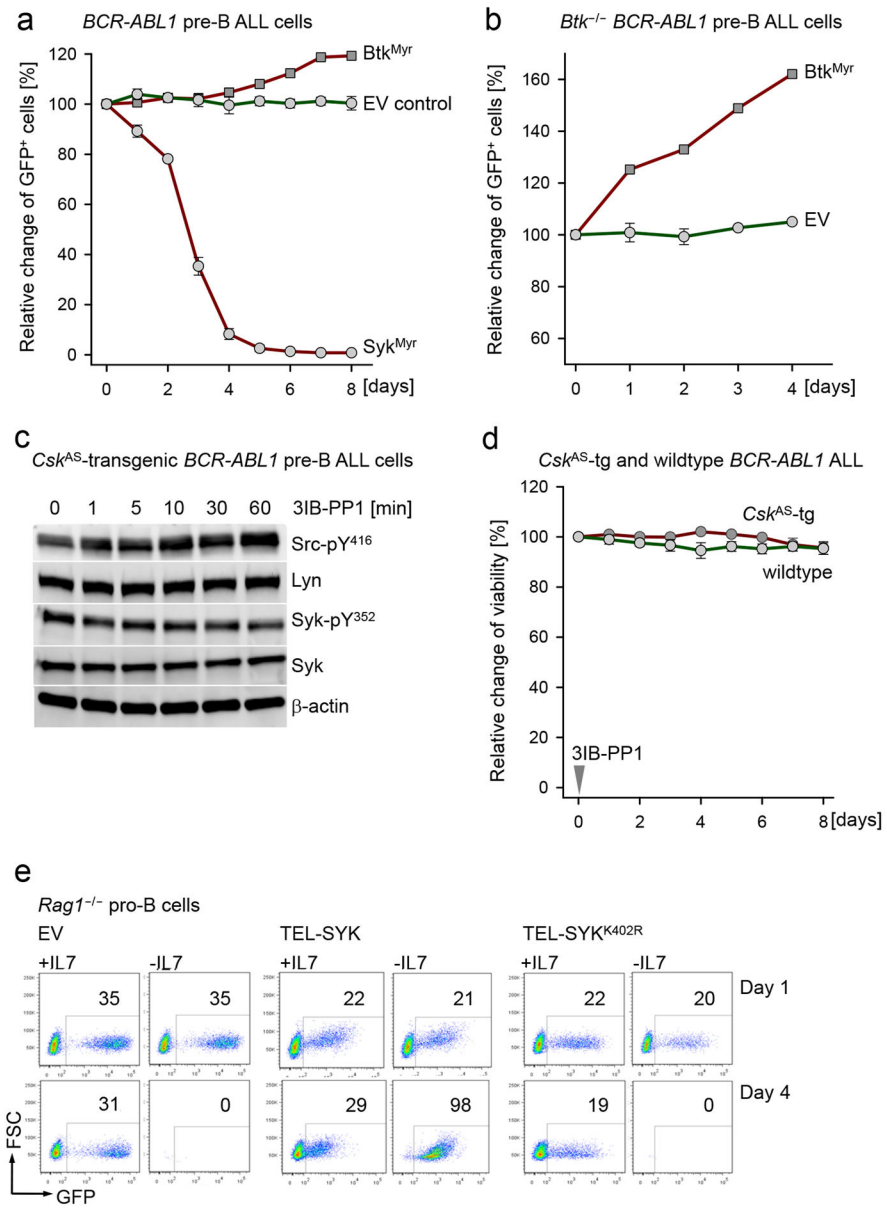


**Extended Data Figure 2. Reconstitution of proximal pre-BCR signaling in pre-B ALL cells**

**a,** *BCR-ABL1* transformed pre-B ALL cells were transduced with myristoylated (active) forms of Btk, Syk or empty vector controls (EV). Vectors were GFP-tagged and fractions of $GFP^+$ cells were monitored over time. **b,** $Btk^{-/-}$ *BCR-ABL1* transformed pre-B ALL cells were transduced with myristoylated (active) Btk or empty vector (both tagged with GFP). Fractions of $GFP^+$ cells were monitored over time. **c,** Csk is a negative regulator of Src family kinase activity. Csk-AS transgenic mice express an analog (3IB-PP1) sensitive form instead of endogenous Csk. For inducible activation of Src kinase activity, we transformed pre-B cells from Csk-AS transgenic mice with *BCR-ABL1*. Addition of 3IB-PP1 (10 μmol/l) released Csk-mediated inhibition and induced increased phosphorylation of Src family kinases at Y416 but not increased Syk-$Y^{352}$ phosphorylation (Western blot). **d,** Pre-B cells

from analog-sensitive Csk-AS transgenic and wildtype mice were transformed with *BCR-ABL1* and treated with 3IB-PP1. Cell viability in response to 3IB-PP1 treatment was monitored over time. Error bars (**a–b, d**) represent mean ± s.d. from three independent experiments. **e,** *Rag1*$^{-/-}$ pro-B cells were expanded in the presence of 10 ng/ml IL7 and transduced with an empty vector (GFP), constitutively active Syk (TEL-SYK-GFP), or kinase dead mutant of SYK (TEL-SYK$^{K402R}$-GFP). Then IL7 was removed from cell cultures and the effect of IL7 removal on cell viability was studied. *Rag1*$^{-/-}$ pro-B cells transduced with EV or TEL-SYK$^{K402R}$-GFP underwent apoptosis, whereas pro-B cells transduced with constitutively active SYK remained viable (not shown). 4 days after IL7-removal, pro-B cells with constitutively active SYK had acquired growth factor (IL7) independence, whereas pro-B cells with EV and TEL-SYK$^{K402R}$-GFP remained dependent on IL7. Data (**c, e**) are representative of three independent experiments.

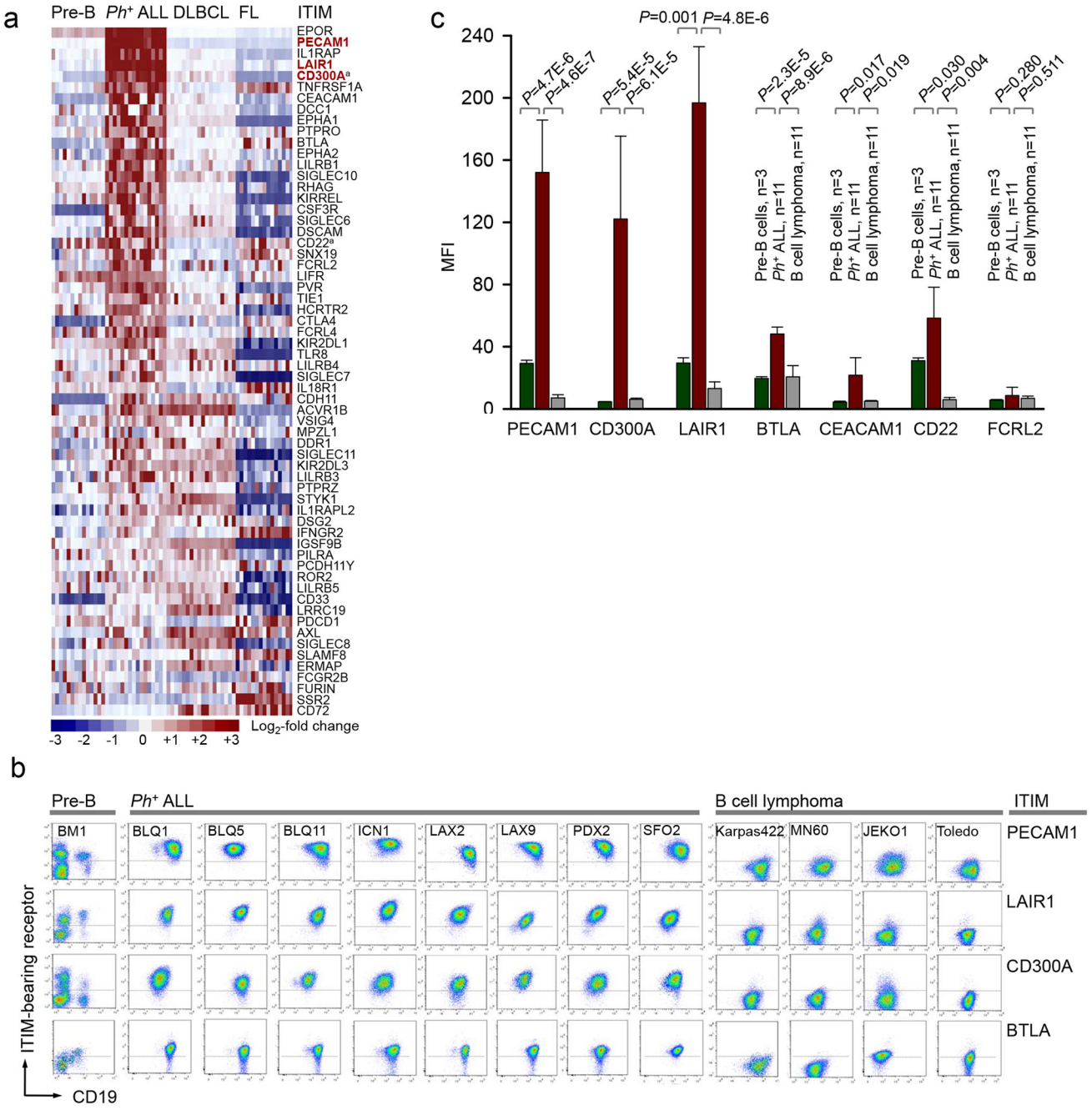


**Extended Data Figure 3. ITIM-bearing receptors are highly expressed on *Ph*$^+$ ALL cells**

**a,** Microarray data for 63 ITIM-bearing receptors are ranked based on the ratio of mRNA levels in *Ph*$^+$ ALL compared to normal pre-B cells and mature B cell lymphomas. **b,** FACS dot plots for double staining of PECAM1, CD300A, LAIR1 and BTLA with CD19 are shown for normal bone marrow pre-B cells (n=1), *Ph*$^+$ ALL cells (n=8) and non-tyrosine kinase B cell leukemia (n=4). **c,** Normal bone marrow mononucleated cells from bone marrow biopsies of healthy donors (n=3), patient-derived *Ph*$^+$ ALL (n=11) and non-tyrosine kinase driven B cell leukemia (n=11) were analyzed by flow cytometry for surface

expression of ITIM-bearing inhibitory receptors PECAM1 (CD31), CD300A (CMRF35), LAIR1 (CD305), BTLA, CEACAM1 (CD66A), CD22 (SIGLEC2), FCRL2 (SPAP1, IRTA4). Additional staining for CD72 and LILRB5 did not show significant differences between $Ph^+$ ALL cells and normal pre-B cells (not shown). Statistical analysis of mean fluorescence intensities (MFI) for normal pre-B cells (n=3), $Ph^+$ ALL (n=11) and non-tyrosine kinase driven B cell lymphoma (n=11) showed significantly increased expression levels of PECAM1, LAIR1 and CD300A in $Ph^+$ ALL compared to normal pre-B cells and non-tyrosine kinase driven B cell leukemia. *P*-values were calculated using unpaired, two-tailed Student's *t*-test.

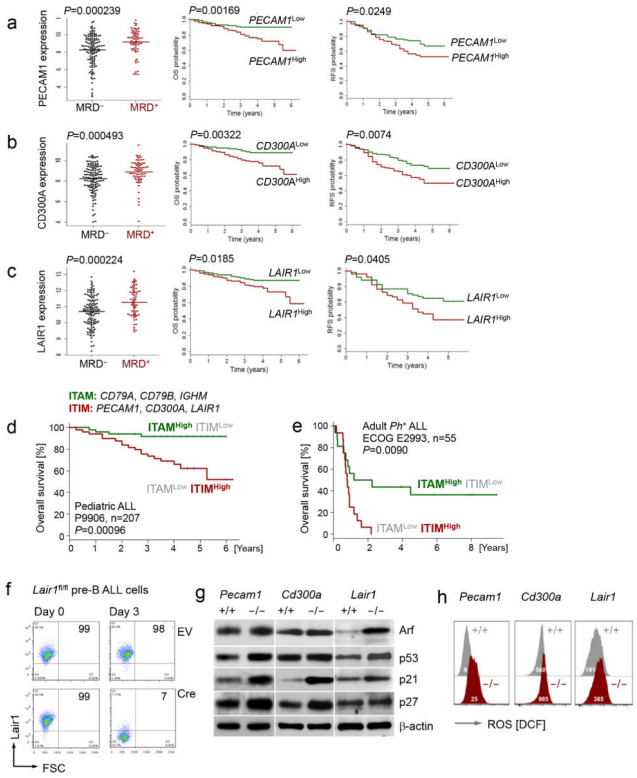


**Extended Data Figure 4. Higher than median expression levels of ITIM-bearing inhibitory receptors predict poor outcomes in patients with pre-B ALL**

**a–c,** mRNA levels for PECAM1, CD300A and LAIR1 were measured in 207 patients with pediatric ALL (COG P9906). PECAM1, CD300A and LAIR1 mRNA levels for ALL cells from 124 patients that had no detectable minimal residual disease (MRD negative; black) on day 29 in their bone marrow were compared to mRNA levels in 67 patients with positive MRD (red) at the time of bone marrow biopsy (day 29). Based on higher or lower-than median expression levels of PECAM1, CD300A and LAIR1, patients were segregated into two groups (High, n=104/Low, n=103; plots in middle and right). Overall survival (OS; middle) and relapse-free survival (RFS; right) probability was estimated by Kaplan-Meier survival analyses. P-values were calculated by Mann-Whitney-Wilcoxon test (left panels; MRD status) and log rank test (middle and right panels; overall survival and relapse-free survival). **d–e,** ITAM-based agonists (CD79A, CD79B, IGHM) and ITIM-based inhibitors

(PECAM1, CD300A, LAIR1) of pre-BCR signaling were combined into a 6-gene outcome predictor based on “ITAM” and “ITIM” signatures and validated in two clinical trials for adults with $Ph^+$ ALL (ECOG E2993) and children with ALL (COG P9906). *P*-values were calculated by log rank test. **f,** *Lair1* deletion was confirmed by flow cytometry. **g,** Expression of checkpoint molecules Arf, p53, p21 and p27 was measured by Western blot in the presence and absence of *Pecam1* and *Cd300a* and upon inducible deletion of *Lair1* in *BCR-ABL1* pre-B ALL cells. **h,** Accumulation of ROS was measured by staining with 2′7′-dichlorofluorescein diacetate (DCF) in *BCR-ABL1* pre-B ALL cells (gray histograms for control; red for gene deletion). Data are representative of three independent experiments (**f–h**).

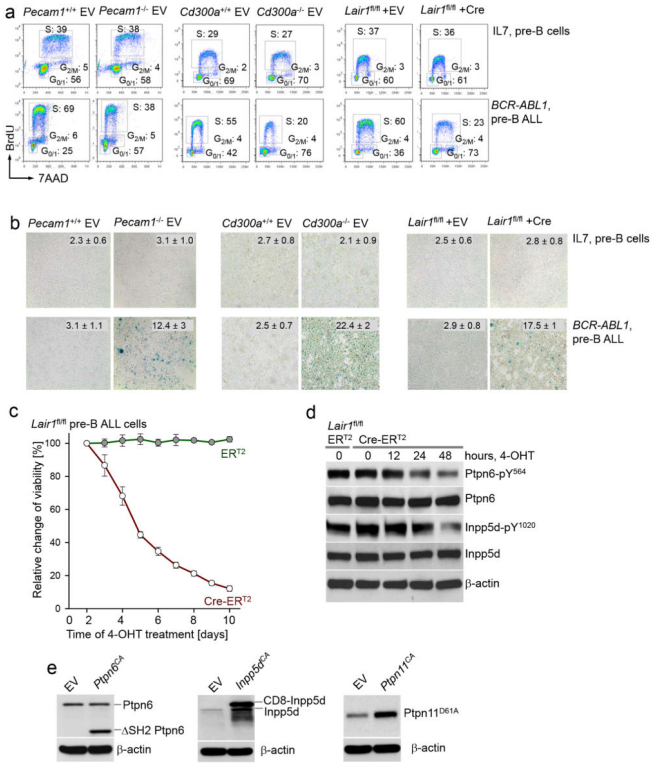


**Extended Data Figure 5. Consequences of genetic deletion of ITIM-bearing receptors in pre-B ALL cells**

**a–b,** B cell precursors from the bone marrow of *Pecam1*$^{-/-}$ and *Cd300a*$^{-/-}$ as well as *Lair1*$^{fl/fl}$ mice and wildtype controls were propagated with IL7 and transduced with an empty vector control (EV; normal B cell precursors) or transformed with *BCR-ABL1* to model $Ph^+$ ALL. Lair1$^{fl/fl}$ pre-B and *BCR-ABL1* leukemia cells were transduced with 4-OHT-inducible retroviral Cre. Cell cycle progression of normal pre-B cells (EV) and *BCR-ABL1* ALL cells was measured by BrdU staining (**a**). Propensity to cellular senescence was measured by staining of normal pre-B and *BCR-ABL1* ALL cells for senescence-associated β-galactosidase (**b**). **c,** *Lair1*$^{fl/fl}$ BCR-ABL1 ALL cells were transduced with 4-OHT-inducible Cre (Cre-ER$^{T2}$) or an empty vector control (ER$^{T2}$). Viability was measured by flow cytometry following 4-OHT treatment. **d,** Effects of inducible deletion of Lair1 on phosphorylation levels of Ptpn6 and Inpp5d were measured by Western blot. **e,** *Lair1*$^{fl/fl}$

ALL cells were transduced with 4-OHT inducible Cre. After antibiotic selection, ALL cells were transduced with a GFP-tagged empty vector control (EV) or GFP-tagged overexpression vectors for constitutively active forms of Ptpn6 (lacking autoinhibitory SH2 domain), Inpp5d (membrane-anchored by CD8) and Ptpn11 (constitutively active D61A mutation). Expression levels of Ptpn6, Inpp5d and Ptpn11 were measured by Western blot using β-actin as loading control. The transduced cells were used for Cre-mediated deletion of *Lair1* to determine if expression of constitutively active Ptpn6, Inpp5d and Ptpn11 can rescue leukemia cell survival. Data (**a, d–e**) are representative of three independent experiments. Error bars (**b–c**) represent mean ± s.d. from three independent experiments.

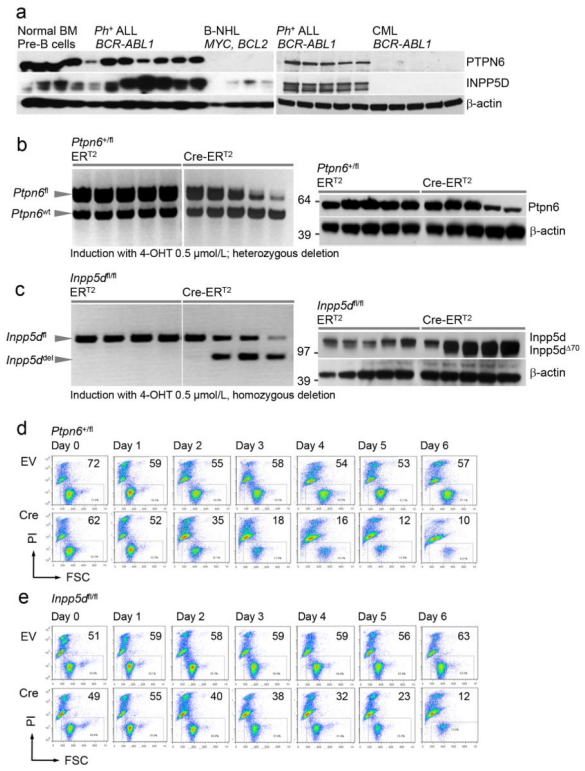


**Extended Data Figure 6. Inducible deletion of *Ptpn6* or *Inpp5d* causes cell death in pre-B ALL cells**

**a,** Protein levels of PTPN6 and INPP5D were measured by Western blot in CD19$^{+}$ bone marrow pre-B cells from healthy donors (n=3), patient-derived *Ph*$^{+}$ ALL (n=8) and B cell leukemia/lymphoma (n=4) lacking an oncogenic tyrosine kinase. Additional Western blot analyses compared expression levels of PTPN6 and INPP5D in patient-derived *Ph*$^{+}$ ALL (n=5) and patient-derived chronic phase CML cells (n=5). **b–c,** Bone marrow cells were isolated from *Ptpn6*$^{+/fl}$ and *Inpp5d*$^{fl/fl}$ mice and pre-B cells were propagated with IL7 (10 ng/ml). *Ptpn6*$^{+/fl}$ and *Inpp5d*$^{fl/fl}$ pre-B cells were then transformed with *BCR-ABL1* retrovirus and subsequently transduced with 4-hydroxy tamoxifen (4-OHT) inducible Cre (Cre-ER$^{T2}$) or an empty vector control (ER$^{T2}$). Addition of 4-OHT induced nuclear translocation of Cre and Cre-mediated excision of *Ptpn6*$^{+/fl}$ (one allele) and *Inpp5d*$^{fl/fl}$ alleles as verified here by genomic PCR (left panels, **b** for *Ptpn6*$^{+/fl}$ and **c** for *Inpp5d*$^{fl/fl}$). Near-complete deletion of the *Ptpn6*$^{+/fl}$ (one allele) and Inpp5d$^{fl/fl}$ floxed alleles was

observed after 3 and 4 days, respectively at the genomic level (left). Kinetics of protein depletion upon heterozygous deletion of *Ptpn6* and homozygous deletion of *Inpp5d* (Inpp5dΔ70) was studied by Western blot (right panels) using β-actin as loading control. **d–e,** Effects of Cre-mediated inducible deletion of *Ptpn6* (**d**) and *Inpp5d* (**e**) on *BCR-ABL1* transformed pre-B ALL cell viability were measured by flow cytometry at the times indicated. Numbers denote percentages of viable cells (determined by forward scatter and propidium iodide uptake). Data are representative of three independent experiments (**d–e**).

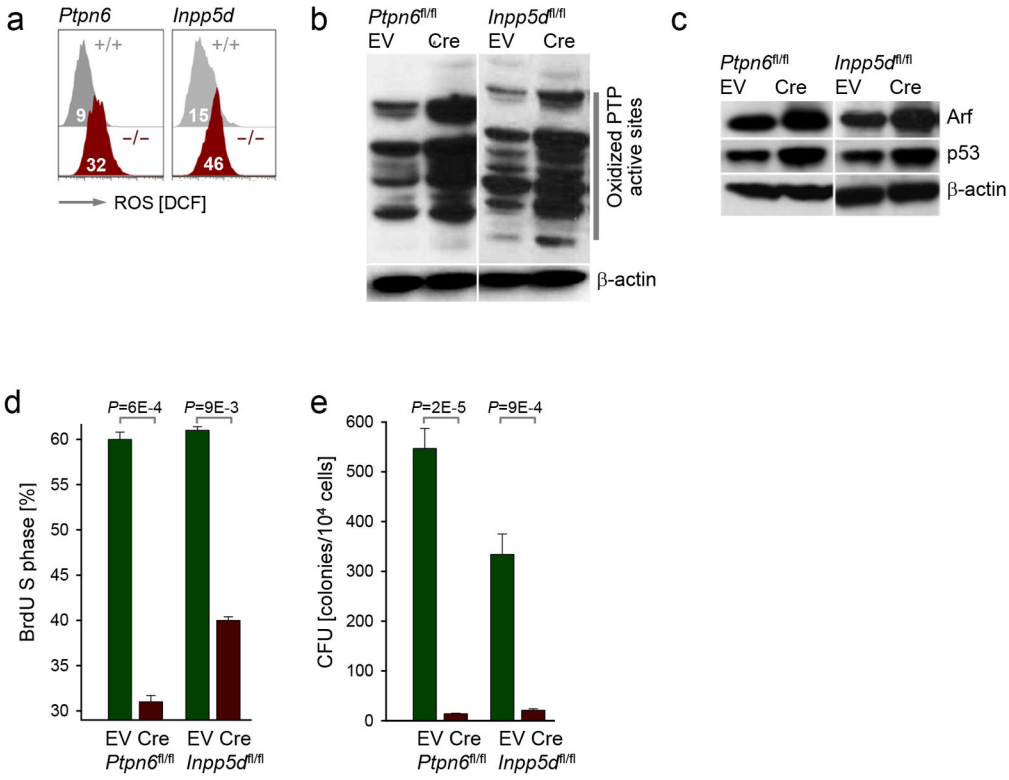


**Extended Data Figure 7. Functional consequences of inducible *Ptpn6* or *Inpp5d* deletion in pre-B ALL cells**

**a,** The effects of deletion of *Ptpn6* and *Inpp5d* on cellular ROS levels were measured by flow cytometry using 2′7′-dichlorofluorescein diacetate (DCF) in *BCR-ABL1* pre-B ALL cells (gray histograms for control; red for gene deletion). **b,** Whether ROS accumulation in response to deletion of *Ptpn6* and *Inpp5d* results in wide-spread cysteine-oxidation and, hence, inactivation, of multiple other PTP active sites was determined by Western blot using antibodies against oxidized PTP active sites. **c,** Protein levels of the checkpoint molecules Arf and p53 were measured by Western blot in *BCR-ABL1* ALL cells before (EV) and after (Cre) deletion of *Ptpn6* and *Inpp5d*. Data are representative of three independent experiments (**a–c**). **d–e,** Functional readouts for inducible deletion of *Ptpn6* and *Inpp5d* include measurement of proliferation (BrdU incorporation; **d**) and colony formation capacity in methylcellulose (CFU assay; **e**). BrdU assays (flow cytometry) and CFU data (images from colonies on plates) are presented in Figure 3d-e. Quantitative and statistical analysis for BrdU incorporation (**d**) and CFU assays (**e**) are depicted here as bar charts. *P*-values

were calculated by unpaired, two-tailed Student's *t*-test. Error bars (**d–e**) represent mean ± s.d. from three independent experiments. Data (**a–c**) are representative of three independent experiments.

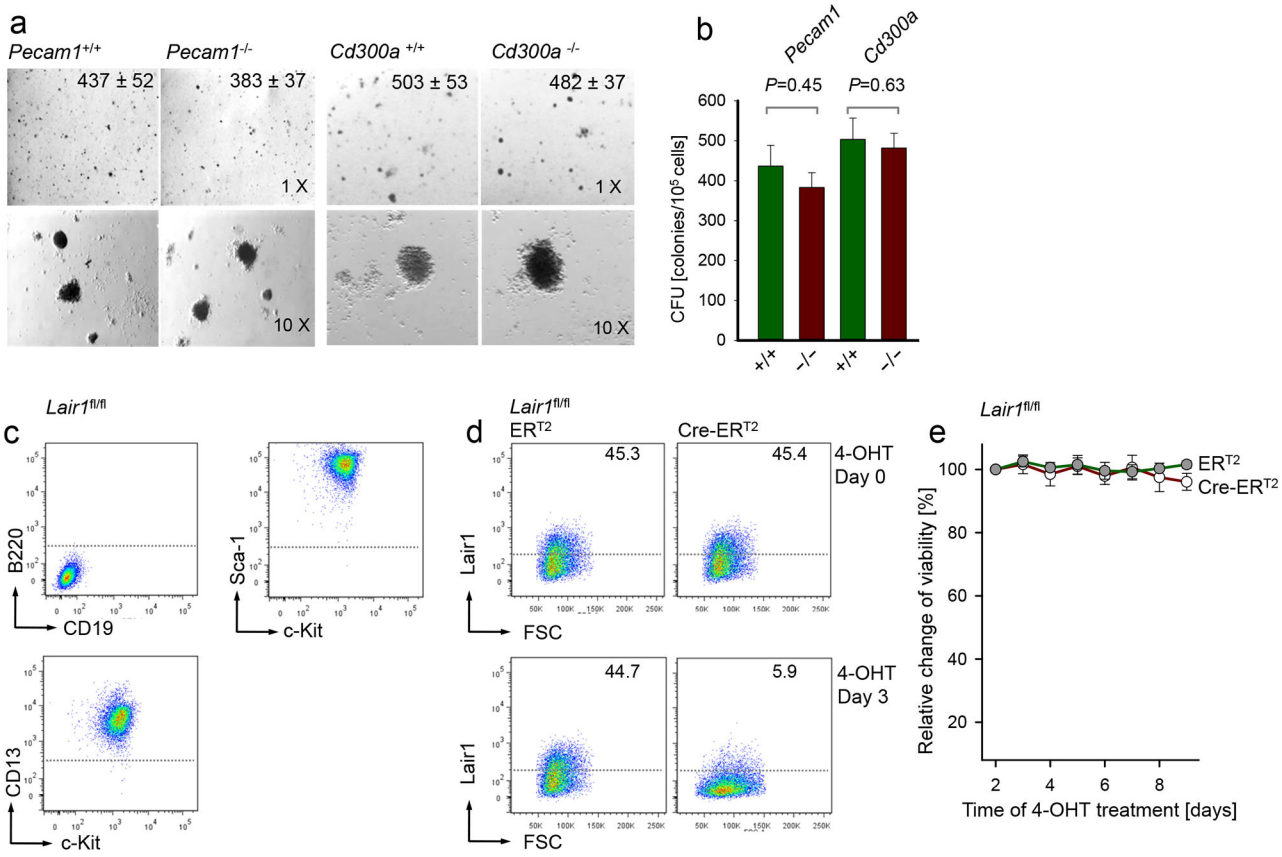


**Extended Data Figure 8. Deletion of ITIM-bearing receptors *Pecam1*, *Cd300a or Lair1* has no significant effects on myeloid CML like cells**

**a–b,** Myeloid progenitor cells from the bone marrow of *Pecam1*$^{-/-}$ and *Cd300a*$^{-/-}$ mice as well as age-matched wildtype controls were propagated in the presence of IL3, IL6 and SCF and transformed with retroviral *BCR-ABL1*. After seven days, outgrowth of myeloid lineage CML-like leukemia was observed. 100,000 *Pecam1*$^{-/-}$ and *Cd300a*$^{-/-}$ CML-like cells as well as wildtype controls were plated in methylcellulose. Colonies were counted two weeks later (**a**). P-values were calculated by unpaired, two-tailed Student's *t*-test (**b**). Data are shown as mean ± standard deviation (s.d.) and representative of three independent experiments (**a–b**). **c–e,** Myeloid progenitor cells from the bone marrow of *Lair1*$^{fl/fl}$ mice were propagated in the presence of IL3, IL6 and SCF and transformed with retroviral *BCR-ABL1*. After seven days, outgrowth of myeloid lineage CML-like leukemia was observed and CML-like phenotype was verified by flow cytometry using antibodies against B220/CD19 (negative), Sca-1/c-kit and CD13 (**c**). CML-like cells were transduced with 4-OHT inducible Cre (Cre-ER$^{T2}$) and empty vector controls (ER$^{T2}$) and deletion of *Lair1* was verified by measurement of Lair1 surface expression (**d**). After adding 4-OHT, cell viability of *Lair1*$^{fl/fl}$ CML cells carrying ER$^{T2}$ or Cre-ER$^{T2}$ was monitored over 9 days by flow

cytometry and is plotted in (**e**). Error bars (**a–b, e**) represent mean ± s.d. from three independent experiments.

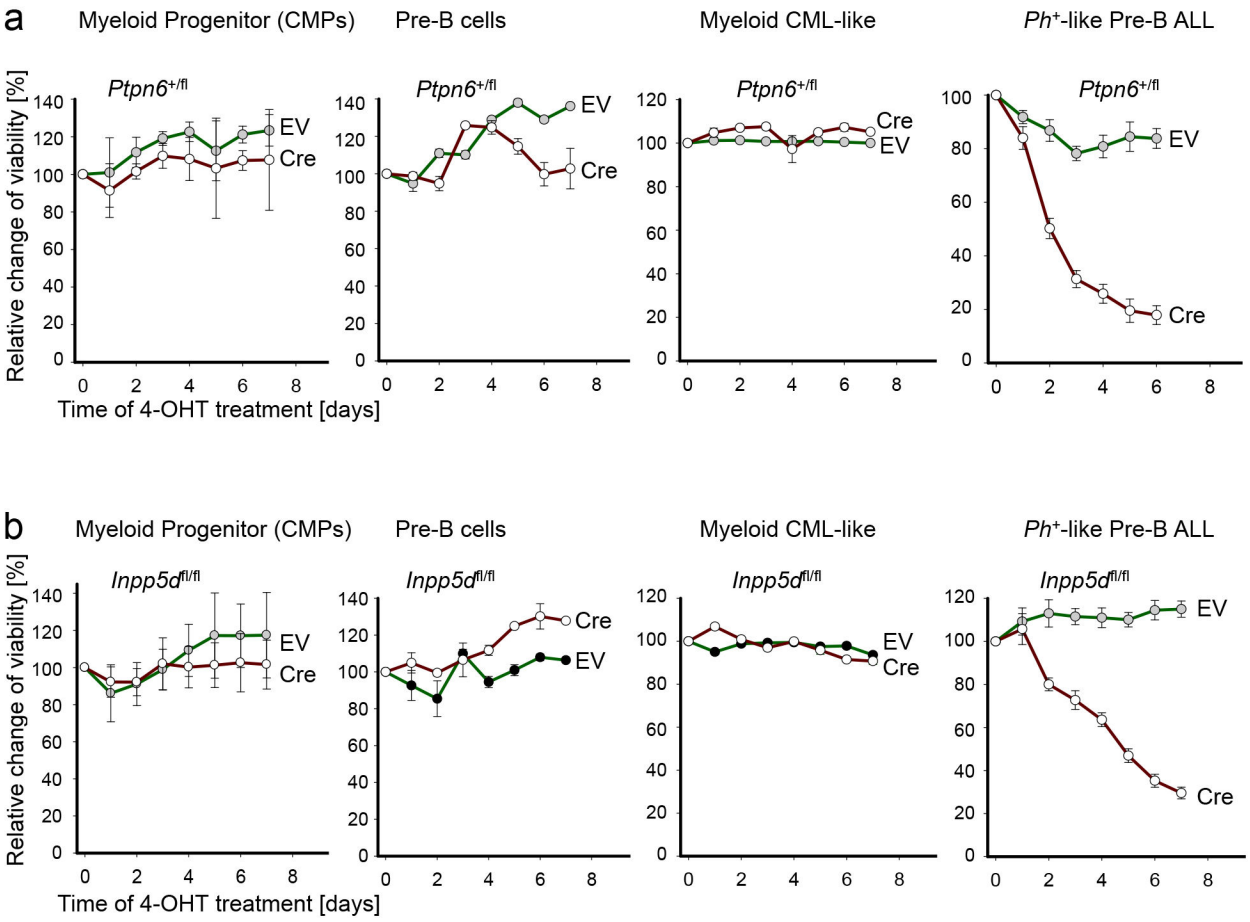


**Extended Data Figure 9. Deletion of *Ptpn6* or *Inpp5d* specifically affects B cell-lineage ALL cells but not normal pre-B cells, myeloid progenitors and myeloid leukemia**

**a–b,** Bone marrow mononuclear cells were isolated from *Ptpn6*$^{+/fl}$ and *Inpp5d*$^{fl/fl}$ mice. Myeloid progenitor cells were propagated with IL6 (25 ng/ml), IL3 (10 ng/ml) and SCF (50 ng/ml) and propagated as common myeloid progenitor cells (CMP) or transformed with *BCR-ABL1* to induce myeloid CML-like leukemia. Pre-B cells were expanded in the presence of IL7 (10 ng/ml) and either propagated as pre-B cell cultured or transformed by *BCR-ABL1* to induce *Ph*$^{+}$ ALL-like leukemia. Lineage identity and >95% purity of cell populations was verified by flow cytometry. *Ptpn6*$^{+/fl}$ and *Inpp5d*$^{fl/fl}$ CMPs, pre-B cells, CML-like and *Ph*$^{+}$ ALL-like leukemia cells were then transduced with 4-hydroxy tamoxifen (4-OHT) inducible Cre (Cre) or an empty vector control (EV). Addition of 4-OHT induced nuclear translocation of Cre and Cre-mediated excision of *Ptpn6*$^{+/fl}$ (one allele; **a**) or *Inpp5d*$^{fl/fl}$ alleles (bottom panel; **b**). Effects of inducible deletion on cell viability were measured by flow cytometry at the times indicated. Error bars (**a–b**) represent mean ± s.d. from three independent experiments.

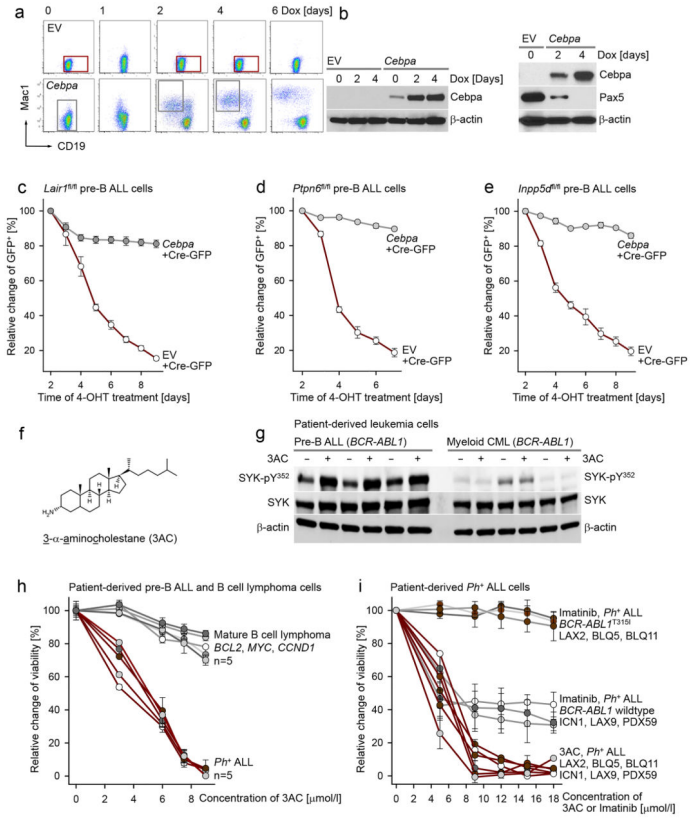


**Extended Data Figure 10. Inhibitory receptor Lair1 and phosphatases Ptpn6, Inpp5d are specifically required by B lineage cells**

**a–b,** B cell lineage *BCR-ABL1* ALL cells were engineered with a doxycycline inducible vector system for expression of Cebpa, which results in downregulation of B cell antigens and myeloid lineage differentiation as measured by flow cytometry (**a**) and Western blot (**b**). Data (**a–b**) are representative of three independent experiments. **c–e,** *BCR-ABL1* driven *Lair1*$^{fl/fl}$, *Ptpn6*$^{fl/fl}$ and *Inpp5d*$^{fl/fl}$ B cell lineage ALL cells (CD19$^{+}$ Mac1$^{-}$) were reprogrammed into myeloid lineage (CD19$^{-}$ Mac1$^{+}$) leukemia cells by addition of doxycycline. Cell cultures were then transduced with 4-OHT inducible GFP-tagged Cre and viability was measured in B cell (gated on CD19$^{+}$ Mac1$^{-}$) and myeloid lineage (gated on CD19$^{-}$ Mac1$^{+}$) populations. **f,** Structure of the INPP5D small molecule inhibitor 3-a-aminocholestane (3AC). **g,** Patient-derived *Ph*$^{+}$ ALL (n=3) and chronic phase CML cells (n=3) were treated with 3AC (10 μmol/l) for 15 minutes, and phosphorylation of SYK was measured by Western blot, using β-actin as loading control. **h,** Dose-response curves are shown for 5 patient-derived cases of ALL (LAX2, LAX9, BLQ1, BLQ5 and PDX2, red curves) and 5 cases of B cell leukemia/lymphoma (lacking an oncogenic tyrosine kinase; KARPAS-422, MHH-PREB-1, JEKO-1, MN-60 and JJN-3, gray curves). **i,** Dose-response curves are shown for the treatment of 6 patient-derived cases of *Ph*$^{+}$ ALL that have acquired global resistance to TKI-treatment (LAX2, BLQ5, BLQ11) or partial resistance (ICN1, LAX9, PDX59). Dose response curves for the TKI Imatinib are shown in gray and for the INPP5D inhibitor 3AC in red (concentration plotted on same scale for both agents). Error bars (**c–e, h–i**) represent mean ± s.d. from three independent experiments.

## Acknowledgments

We thank Dr. Rudi W. Hendriks (Erasmus University, Rotterdam, Netherlands) for encouragement and critical discussions, Angela Park and Carrie Lin and all members of the Müschen laboratory, Dr. Linjie Tian (Coligan laboratory) and Bethany Scott (Bolland laboratory) for their support. This work is supported by grants from the NIH/NCI through R01CA137060, R01CA139032, R01CA169458, R01CA172558 and R01CA157644 (to M.M.), ECOG-ACRIN grants CA180820 and CA180794 (to E.P.), grants from the Leukemia and Lymphoma Society (to M.M.), the California Institute for Regenerative Medicine through TR02-1816 (M.M.), the William Lawrence and Blanche Hughes Foundation. M.M. is a Scholar of The Leukemia and Lymphoma Society and a Senior Investigator of the Wellcome Trust.

## Abbreviations

| | |
|---|---|
| **3AC** | 3-α-aminocholestane |
| **4-OHT** | 4-hydroxytamoxifen |
| **ALL** | acute lymphoblastic leukemia |
| **BCR** | B cell receptor |
| **DCF-DA** | 2′7′-dichlorofluorescein diacetate |
| **EV** | empty vector |
| **IL** | Interleukin |
| **MFI** | mean fluorescence intensity |
| **ITAM** | immunoreceptor tyrosine-based activation motif |
| **ITIM** | immunoreceptor tyrosine-based inhibitory motif |
| **LMP2A** | latent membrane protein 2A |
| **MRD** | minimal residual disease |
| **n** | denotes the number of independent experiments |
| **OS** | overall survival |
| **Ph** | Philadelphia chromosome |
| **RFS** | relapse-free survival |
| **TKI** | tyrosine kinase inhibitor |

## References

1. Lam KP, Kühn R, Rajewsky K. In vivo ablation of surface immunoglobulin on mature B cells by inducible gene targeting results in rapid cell death. Cell. 1997; 90:1073–1083. [PubMed: 9323135]
2. Nemazee DA, Bürki K. Clonal deletion of B lymphocytes in a transgenic mouse bearing anti-MHC class I antibody genes. Nature. 1989; 337:562–566. [PubMed: 2783762]
3. Keenan RA, et al. Censoring of autoreactive B cell development by the pre-B cell receptor. Science. 2008; 321:696–699. [PubMed: 18566249]
4. Klein F, et al. The BCR-ABL1 kinase bypasses selection for the expression of a pre-B cell receptor in pre-B acute lymphoblastic leukemia cells. The Journal of experimental medicine. 2004; 199:673–685. [PubMed: 14993251]
5. Feldhahn N, et al. Mimicry of a constitutively active pre-B cell receptor in acute lymphoblastic leukemia cells. The Journal of experimental medicine. 2005; 201:1837–1852. [PubMed: 15939795]

6. Cortes JE, et al. Ponatinib in refractory Philadelphia chromosome-positive leukemias. The New England journal of medicine. 2012; 367:2075–2088. [PubMed: 23190221]
7. Pao LI, et al. B cell-specific deletion of protein-tyrosine phosphatase Shp1 promotes B-1a cell development and causes systemic autoimmunity. Immunity. 2007; 27:35–48. [PubMed: 17600736]
8. O'Neill SK, et al. Monophosphorylation of CD79a and CD79b ITAM motifs initiates a SHIP-1 phosphatase-mediated inhibitory signaling cascade required for B cell anergy. Immunity. 2011; 35:746–756. [PubMed: 22078222]
9. Brooks R, et al. SHIP1 inhibition increases immunoregulatory capacity and triggers apoptosis of hematopoietic cancer cells. Journal of immunology. 2010; 184:3582–3589.
10. Roberts KG, et al. Targetable kinase-activating lesions in Ph-like acute lymphoblastic leukemia. New England journal of medicine. 2014; 371:1005–1015. [PubMed: 25207766]
11. Duy C, et al. BCL6 enables Ph+ acute lymphoblastic leukaemia cells to survive BCR-ABL1 kinase inhibition. Nature. 2011; 473:384–388. [PubMed: 21593872]
12. Reth M. Antigen receptor tail clue. Nature. 1989; 338:383–384. [PubMed: 2927501]
13. Anderson LJ, Longnecker R. EBV LMP2A provides a surrogate pre-B cell receptor signal through constitutive activation of the ERK/MAPK pathway. The Journal of general virology. 2008; 89:1563–1568. [PubMed: 18559925]
14. Kulathu Y, Grothe G, Reth M. Autoinhibition and adapter function of Syk. Immunological reviews. 2009; 232:286–299. [PubMed: 19909371]
15. Bolland S, Ravetch JV. Inhibitory pathways triggered by ITIM-containing receptors. Advances in immunology. 1999; 72:149–177. [PubMed: 10361574]
16. Staub E, Rosenthal A, Hinzmann B. Systematic identification of immunoreceptor tyrosine-based inhibitory motifs in the human proteome. Cellular signalling. 2004; 16:435–456. [PubMed: 14709333]
17. Limnander A, et al. STIM1, PKC-δ and RasGRP set a threshold for proapoptotic Erk signaling during B cell development. Nature immunology. 2011; 12:425–433. [PubMed: 21441934]
18. Zhang SQ, et al. Shp2 regulates SRC family kinase activity and Ras/Erk activation by controlling Csk recruitment. Molecular cell. 2004; 13:341–355. [PubMed: 14967142]
19. Meng TC, Fukada T, Tonks NK. Reversible oxidation and inactivation of protein tyrosine phosphatases in vivo. Molecular cell. 2002; 9:387–399. [PubMed: 11864611]
20. Bolland S, Pearse RN, Kurosaki T, Ravetch JV. SHIP modulates immune receptor responses by regulating membrane association of Btk. Immunity. 1998; 8:509–16. [PubMed: 9586640]
21. Xie H, Ye M, Feng R, Graf T. Stepwise reprogramming of B cells into macrophages. Cell. 2004; 117:663–676. [PubMed: 15163413]
22. Mullighan CG, et al. BCR-ABL1 lymphoblastic leukaemia is characterized by the deletion of Ikaros. Nature. 2008; 453:110–114. [PubMed: 18408710]
23. Li S, Ilaria RL, Million RP, Daley GQ, Van Etten RA. The P190, P210, and P230 forms of the BCR/ABL oncogene induce a similar chronic myeloid leukemia-like syndrome in mice but have different lymphoid leukemogenic activity. The Journal of experimental medicine. 1999; 189:1399–1412. [PubMed: 10224280]

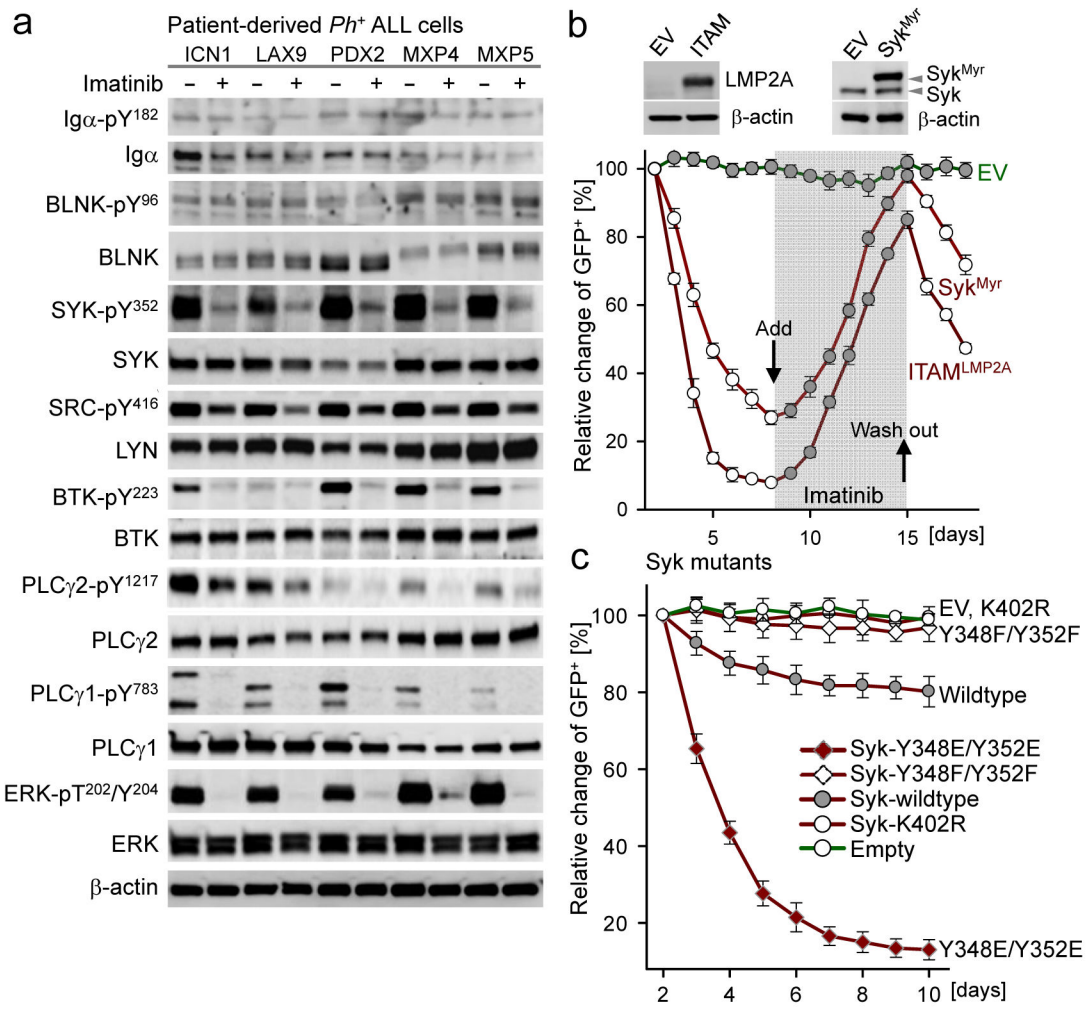


**Figure 1. Reconstitution of defective ITAM-signaling induces cell death in BCR-ABL1 ALL cells**

**a,** Patient-derived *Ph*$^{+}$ ALL cells were treated with or without imatinib (10 μmol/l) for 6 hours and phosphorylation of Igα, SLP-65 (BLNK), SYK, SRC, BTK, PLCγ2, PLCγ1 and ERK1/2 was measured by Western blot (n=5). **b,** *BCR-ABL1* ALL cells transduced with GFP-tagged LMP2A-ITAM, SYK$^{Myr}$ or an EV were monitored over time in the presence or absence of 0.5 μmol/l imatinib by flow cytometry. The expression level of LMP2A and SYK$^{Myr}$ were measured by Western blot. **c,** *BCR-ABL1* ALL cells were transduced with GFP-tagged wildtype SYK or SYK mutant vectors (Y348E/Y352E, Y348F/Y352F, K402R) or an EV and relative changes of transduced (GFP$^{+}$) cells were monitored by flow cytometry. Data are presented as means ± standard deviation (s.d.) from three independent experiments (**b–c**).

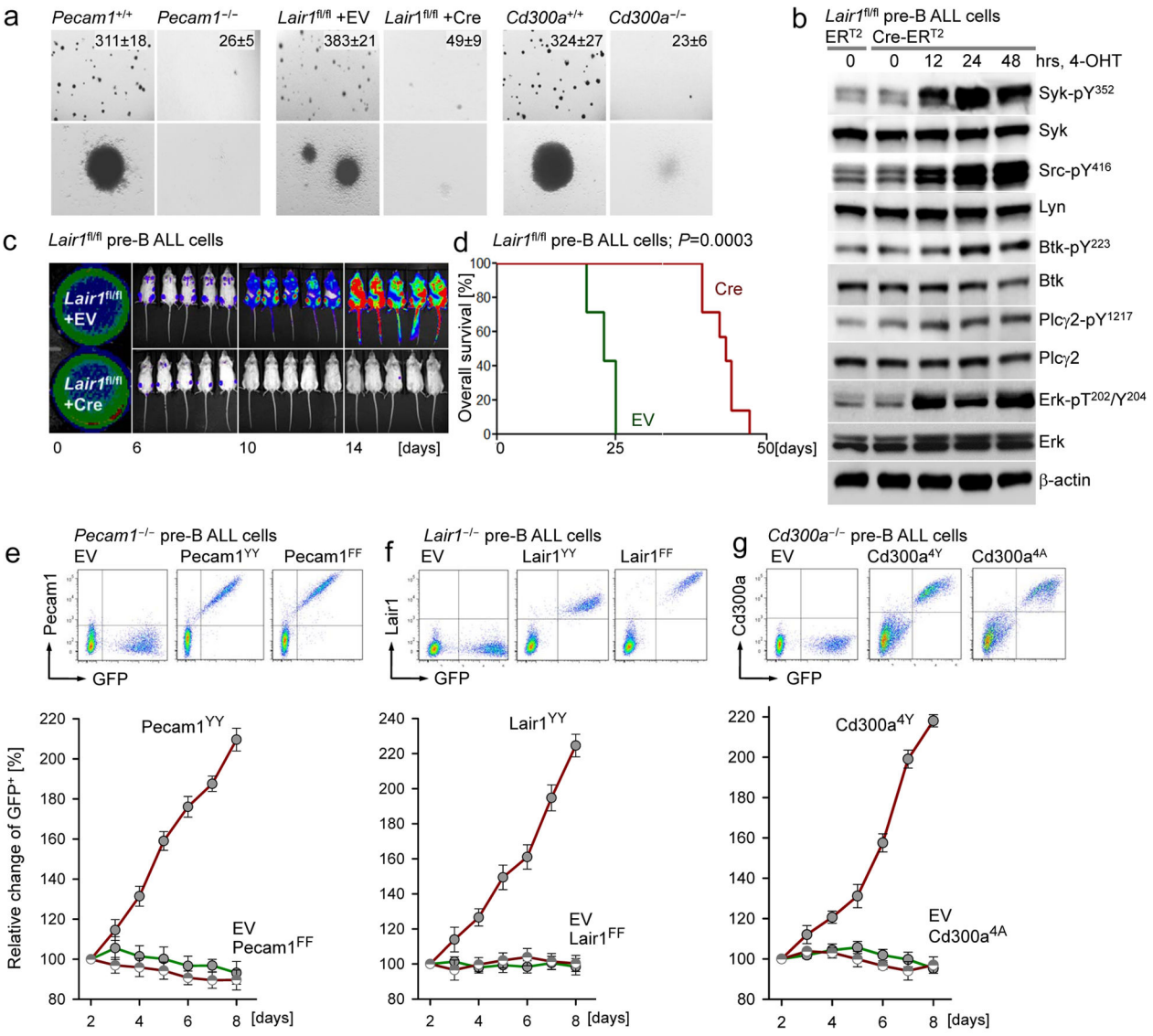


**Figure 2. Inhibitory ITIM-bearing receptors are critical for pre-B leukemogenesis**

**a,** Pre-B cells from *Pecam1*$^{-/-}$, *Cd300a*$^{-/-}$, *Lair1*$^{fl/fl}$ mice and wildtype controls were propagated with IL7 and transduced with *BCR-ABL1*. *Lair1*$^{fl/fl}$ ALL cells were transduced with 4-OHT-inducible Cre. Colony formation assays were performed, showing photomicrographs of colonies at 1x and 10x magnification. **b,** Effects of inducible deletion of *Lair1* on phosphorylation levels of Syk, Src, Btk, Plcγ2 and Erk were measured by Western blot. Data are representative of three independent experiments. **c,** *Lair1*$^{fl/fl}$ ALL cells were labeled with firefly luciferase, transduced with 4-OHT-inducible Cre or empty vector control (EV), treated with 4-OHT for 24 hours and transplanted into sublethally irradiated NOD/SCID mice and leukemia burden was measured by luciferase bioimaging. **d,** A Kaplan-Meier analysis compared overall survival of transplant recipients in the two groups (n=7 for each group). *P* value was calculated by log-rank test. **e–g,** *Pecam1*$^{-/-}$, *Lair1*$^{-/-}$ (4-OHT-induced deletion) and *Cd300a*$^{-/-}$ pre-B cells were reconstituted with wildtype, Pecam1$^{FF}$ (Y679F/Y702F), Lair1$^{FF}$ (Y228F/Y257F), Cd300a$^{4A}$ (Y231A/Y255A/

Y267A/Y293A) mutant vectors or EV, and then transformed by BCR-ABL1. The expression levels of wildtype or mutant receptors were monitored by flow cytometry. Data are presented as means ± s.d. from three independent experiments (**a, e–g**).

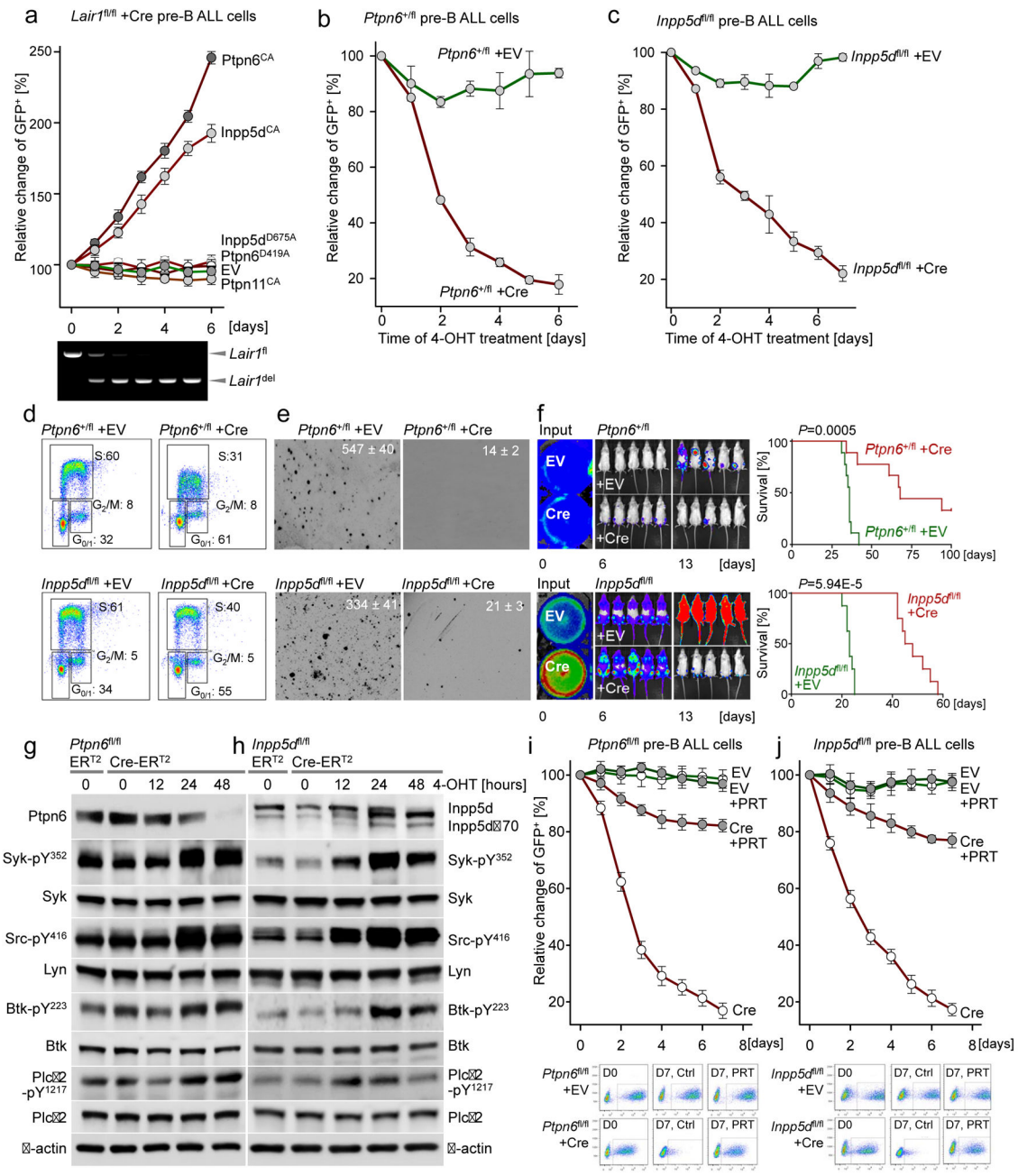


**Figure 3. ITIM-dependent activation of Ptpn6 and Inpp5d phosphatases enables pre-B leukemogenesis**

**a,** *Lair1*$^{fl/fl}$ ALL cells were transduced with 4-OHT inducible Cre. After antibiotic selection, leukemia cells were transduced with GFP-tagged empty vector (EV) or overexpression vectors for constitutively active (CA) forms of *Ptpn6* (SH2 domain deleted), *Inpp5d* (CD8-*Inpp5d*), Ptpn11 (*Ptpn11*$^{D61A}$), or phosphatase-inactive mutants (*Ptpn6*$^{D419A}$, *Inpp5d*$^{D675A}$). After addition of 4-OHT, Cre-mediated deletion of *Lair1* was monitored by PCR. Percentages of GFP$^{+}$ cells were measured by flow cytometry. **b–c,** Inducible activation of Cre in *Ptpn6*$^{+/fl}$ (**b**) and *Inpp5d*$^{fl/fl}$ (**c**) *BCR-ABL1*-transformed ALL cells

resulted in depletion of transduced cells. **d–e,** Effects of deletion of *Ptpn6* and *Inpp5d* on proliferation (cell cycle analysis, BrdU; **d**) and colony formation ability (**e**) were measured. **f,** *Ptpn6*$^{+/fl}$ and *Inpp5d*$^{fl/fl}$ ALL cells carrying 4-OHT inducible Cre (Cre) or EV were labeled with firefly luciferase, treated with 4-OHT for 24 hours and injected into NOD/SCID mice. Overall survival of the two groups of recipient mice (EV, Cre; n=8 per group) was studied by Kaplan-Meier analysis, *P* values calculated by log-rank test. **g–h,** Effects of deletion of *Ptpn6* (**g**) and *Inpp5d* (**h**) on phosphorylation of Syk, Src, Btk, Plcγ2 were measured by Western blot. **i–j,** *Ptpn6*$^{fl/fl}$ and *Inpp5d*$^{fl/fl}$ ALL cells carrying 4-OHT inducible Cre (Cre) or an empty vector (EV) were pre-treated with the SYK inhibitor PRT06207 (2.5 μmol/l) for two days. Deletion of *Ptpn6* (**i**) or *Inpp5d* (**j**) was induced by addition of 4-OHT and relative changes of GFP$^{+}$ cells were monitored by flow cytometry. BrdU and Western blot data are representative of three independent experiments (**d, g–h**). Error bars (**a–c, e, i–j**) represent mean ± s.d. from three independent experiments.

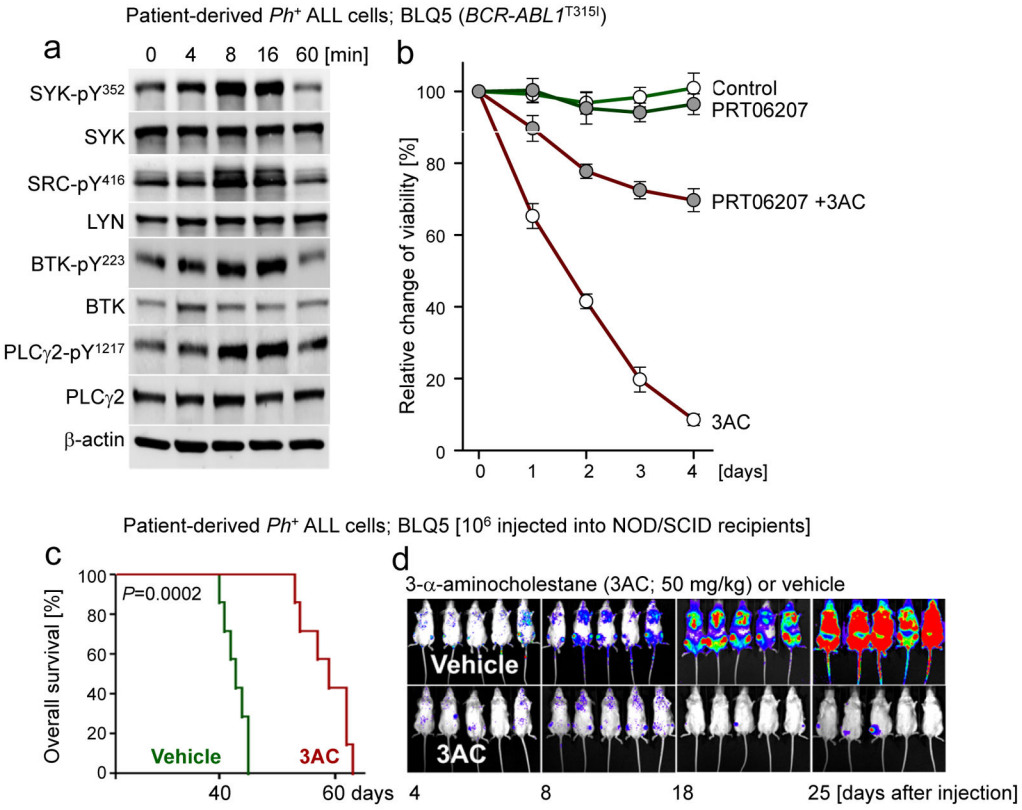


**Figure 4. Small molecule inhibition of Inpp5d induces hyperactivation of Syk and triggers a deletional checkpoint in pre-B ALL cells**

**a,** Patient-derived *Ph*$^+$ ALL cells (BLQ5) were treated with 3AC (10 μmol/l) for the times indicated and phosphorylation of SYK, SRC, BTK, PLCγ2 were measured by Western blot. Data are representative of three independent experiments. **b,** ALL cells were treated with vehicle, Syk inhibitor PRT (2.5 μmol/l), 3AC (7.5 μmol/l) alone, or pre-treated with PRT for 2 days and then added 3AC. Viability was monitored by flow cytometry. Error bars represent mean ± s.d. from three independent experiments. **c–d,** TKI-resistant patient-derived *Ph*$^+$ ALL cells (BLQ5) were labeled with firefly luciferase and injected into sublethally irradiated NOD/SCID mice, treated with either 3AC or vehicle (50 mg/kg, ip injection daily, n=7 per group). Overall survival of recipient mice in the two groups was compared by Kaplan-Meier analysis (**c;** *P* value calculated by log-rank test) and leukemia burden was measured by luciferase bioimaging (**d**).